Shape and faceting of Si nanocrystals embedded in a-SiO_2: A Monte Carlo study

G. Hadjisavvas, I. N. Remediakis, and P. C. Kelires
Physics Department, University of Crete, P.O. Box 2208, 710 03, Heraclion, Crete, Greece
(Received 21 July 2006; revised manuscript received 25 September 2006; published 25 October 2006)

We study the equilibrium shape and faceting of Si nanocrystals embedded in a-SiO_2, using continuous-space Monte Carlo simulations supplemented by the Wulff construction method. Our aim is to explain in atomistic terms why large nanocrystals are often observed to be faceted, while smaller ones are always found to be spherical. By developing and analyzing realistic structural models, we show that faceting is indeed the equilibrium state of large nanocrystals, and that it breaks down as the size shrinks. The decomposition of interface energies into bond contributions reveals that the key factors driving the destabilization of facets are the distortions of Si-O-Si bridge bonds at the edges and apeces of the unstable facets. The transition region from a faceted to a spherical shape is in the range of 4–6 nm.

DOI: 10.1103/PhysRevB.74.165419 PACS number(s): 61.46.Hk, 68.35.Ct, 68.35.Md

I. INTRODUCTION

One of the fundamental issues in the study of semiconductor nanocrystals (NCs) concerns the control of their shape attained during growth.[1] Depending on the conditions, NCs either obtain a spherical shape without facets or develop well defined facets and a polyhedral shape. Faceting is a phenomenon of not only basic interest, but it has practical consequences as well. For example, it may play an important role in controlling the optoelectronic properties, such as doping efficiency[2] and light emission.

Faceting may be viewed as the result of minimization of surface tension at thermodynamic equilibrium. Due to the different number of dangling bonds and different reconstructions, certain semiconductor surfaces have lower energy and are more stable than others. In the simple case of free-standing (isolated) NCs, the formation of facets with low surface energy is naturally favored. However, this is not so obvious and transparent when the NCs are embedded in a host matrix in order to provide rigidity, suspension, and insulation. In this case, the reconstructions of the free surfaces do not exist, while the bonding geometries at the formed interfaces are often quite complex.

A prototypical example is offered by Si-NC embedded in a-SiO_2, a nanocomposite system extensively studied in the literature as a candidate for efficient light emission[3] and as a charge storage element in nonvolatile memory devices.[4] A number of experimental works have shown[5–7] that NC with sizes (diameter) larger than ~5 nm develop, but not always, well-defined facets, while smaller ones always grow spherical, without facets.

The central question which arises is why faceting is favored for large NC, and why it breaks down for smaller ones at the reported transition region. Qualitative arguments given in the literature assume that the spherical shape minimizes strain in small NC.[6] This implies that the interface facets cannot be sustained because it costs strain energy to do so. However, it is not clear how the facets become unstable, and how strain minimization is achieved by having a spherical interface. To understand this phenomenon, the atomistic mechanisms causing the destabilization and the interface elements responsible for the defaceting have to be exposed, including disorder and bonding effects.

Here, we report direct simulations which are able to unravel the energetics and the atomistics of the faceting-defaceting transition in Si-NC/a-SiO_2. This is made possible by using realistic structural models of faceted and spherical embedded NC, obtained by a state-of-the-art Monte Carlo (MC) approach. By extracting and analyzing the interface energies, and by decomposing them into contributions from various geometries, we are able to show that the key factor driving the faceting-defaceting transition are the distortions of Si-O-Si bridge bonds at the edges and apeces of the faceted interface, and much less the chemical disorder.

The paper is organized as follows. Section II briefly describes the methodology used in this work. Sections III A and III B report the interface energies of various planar c-Si/a-SiO_2 structures and the optimum shape of an embedded Si-NC, respectively. A comparison between a small and a large Si-NC is done in Sec. III C. Finally, the conclusions of this work are given in Sec. IV.

II. METHODOLOGY

Our approach consists of three steps. We first construct a number of planar c-Si/a-SiO_2 interfaces of different orientations and calculate their energies and other properties. Based on these energies, we perform in the second step a Wulff construction analysis, in order to predict the equilibrium NC shape and facets. In the third step, the so obtained faceted Si-NC, as well as spherical ones of the same size, are embedded in the oxide to find out which structures, and for what reason, are stable or unstable at both the large and small size regimes.

The employed MC methodology has been recently applied with success[8] to the study of the interface structure, energetics, and distortions of small spherical Si-NC/a-SiO_2. In this method, the Si/a-SiO_2 system is modeled as a defect-free network in which Si and O have four and two bonds, respectively, without any O-O bonds. The energies are reasonably approximated by a Keating-like valence force model,[9] which is composed by a term representing the cost for bond-length and bond-angle distortions (strain energy), and a second term representing the chemical energy cost for the formation of suboxides.

For both planar c-Si/a-SiO_2 and curved Si-NC/a-SiO_2 interfaces, the amorphous oxide is generated using the well established MC algorithm of Wooten, Winer, and Weaire (WWW),[10] involving bond breaking and switching moves. Compositional equilibration of the interface is achieved by bond conversion moves,[8] exchanging a Si-Si bond in the c -Si part of the system with a neighboring Si-O-Si bond in the oxide. Volume relaxation moves serve as to relieve the stress in the entire system. For all types of moves, acceptance or rejection is decided according to the Metropolis criterion.

To actually generate the composite systems, we follow the procedure outlined in detail in Ref. 8. The starting point are periodic cells in the β-crystobalite structure. For the planar case, tetragonal cells with layers of a given orientation are used, with the lateral dimensions fixed at the Si lattice constant. By removing the O atoms within a predetermined thick slab layer, an all-Si region is formed to simulate the Si substrate. Similarly, for the Si-NC case, where we use cubic cells, the NC is formed by removing the O atoms from a spherical or polyhedral region, at the center of the cell, depending on whether the simulated NC is spherical or faceted. In both cases, the removal of O atoms is followed by a relaxation of these unphysical starting geometries to their energy minimum. Then, in a second stage, the amorphous oxide matrix is generated and topologically equilibrated by the WWW procedure, and the interfaces are compositionally equilibrated by bond conversion MC moves. Amorphization and equilibration (see Ref. 8) lasts for more than 4×10^6 moves. Properties are calculated by taking averages at 0.1 eV (887 °C) over 1×10^6 MC steps.

III. RESULTS

A. Interface energies

We have generated in total six fully relaxed planar c -Si/a-SiO_2 structures with different interface orientations. They are portrayed in Fig. 1. For each structure, we calculate the interface energy E_{inter}, defined as the difference between the total energy of the cell and the sum of the bulk energies of the amorphous oxide and crystalline Si; the suboxide components; the interface width σ,[8,9] indicating the dispersion of suboxides at the interface; the percentage of Si-O-Si bridge bonds, in which an O atom connects two Si atoms terminating the c-Si region; and their energy E_{bridge} obtained by decomposing the total energy of the system into individual bond contributions. Bridge bonds were previously shown to be the lowest-energy structural element at the planar c -Si(100)/a-SiO_2 interface,[9,11] because they can be stretched and bent with minimal energy cost. Here, we also examine their stability on orientations other than the (100). All above properties are summarized in Table I.

Overall, the interface energies are determined by a competition between the low-energy bridge bonding, the suboxide penalty, and the abruptness of the interface, with the former being the dominant factor. We find that the (100) interface, composed of 100% bridge bonds, is by far the lowest-energy interface, because bridges on this orientation have lower energy, by at least 0.2 eV, than on any other orientation, and because it is more abrupt (smaller width).

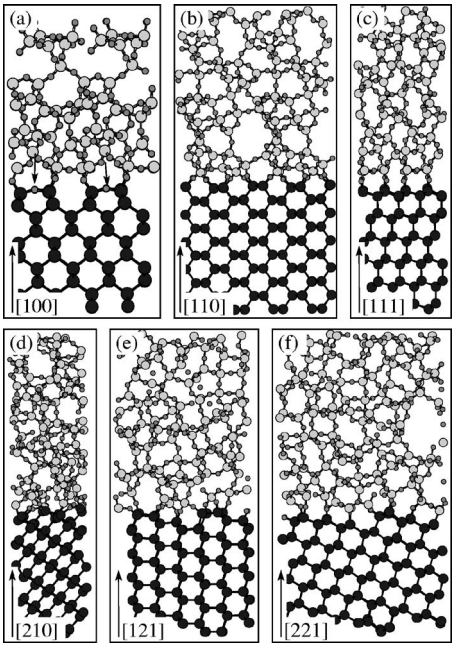

FIG. 1. Ball and stick models of six different planar Si/a-SiO_2 interfaces. (a)–(g): the (100), (110), (111), (210), (121), and (221) orientations. Dark spheres show Si atoms in the crystalline region. Small grey spheres and light grey spheres denote O and Si atoms in the oxide, respectively. Arrows in (a) indicate the formation of bridge bonds.

We take its E_{inter} (0.046 eV/Å^2) as a reference. The low energy of bridges is associated to small distortions, as bond lengths and angles involved are close to their nominal values (1.6 Å, ~145°). The next low-energy structure is the (121) interface, despite having a large σ, because of lower bridge and normal Si-O-Si bond energies than in other orientations. (In normal Si-O-Si interface bonds, an O atom connects a Si atom in the c-Si region with a Si atom in the oxide.) The (110) and (111) interfaces, with no bridge bonds, are found to be degenerate in energy, as a result of cancelling contributions, but still close to the (121) due to the low values of σ. The (210) and (221) interfaces, on the other hand, have high energies, due to bridge distortions and wide spread of suboxides.

B. Optimum NC shape

In the second step, based on these energies, we construct the most probable (equilibrium) NC shape which minimizes the interface energy for a given enclosed volume. We use the Wulff construction method.[12] The main steps are the following. Starting from an arbitrary point O, one draws vectors in the direction of all possible crystallographic faces $\hat{n}$, with magnitude $E_{\text{inter}}(\hat{n})$, where $E_{\text{inter}}(\hat{n})$ is the absolute energy of the interface with orientation $\hat{n}$. A plane normal to each such vector is drawn passing through its tip. The inner envelope of all these planes (the enclosed polyhedron) is the Wulff shape. Only planes that are part of the Wulff construction are thermodynamically stable.

The optimum shape for an embedded NC, as revealed by this analysis, is shown in Fig. 2. It is a polyhedron composed

TABLE I. Percentage of bridge bonds, ratios of oxidation states, interface widths σ (Å), energies of bridge bonds E_{bridge} (eV), and interface energies E_{inter} (eV/Å^2) for various orientations. The (100) orientation is taken as a reference.

	(100)	(110)	(111)	(210)	(121)	(221)
% bridges	100	0	0	83	60	59
$Si^{+1}:Si^{+2}:Si^{+3}$	0:1:0	1:0:0	1:0:0	1:1:1	3:2:1	1:0:1
σ	0.08	0.12	0.10	0.61	0.57	0.58
E_{bridge}	0.00			0.25	0.21	0.31
E_{inter}	0.000	0.010	0.010	0.061	0.005	0.050

of 42 facets. Only three different orientations exist: the (100), (110), and (121), with 6, 12, and 24 facets, respectively. The facet areas are proportional to the ordering of the energies, so (100) has the largest and (110) the smallest facets. Note that, as a result of the construction process, facets with the (111) orientation have negligible contribution and very small area, and thus do not appear, although degenerate with (110). However, because of the subtle energy differences involved, the accuracy of the Keating potential is probably not enough to unambiguously decide on this, and we should not exclude the presence of (111) facets as experimentally proposed.[5,6] Also, although we limited our search for stable facets to low-index interfaces, we do not exclude the existence of stable facets with indices higher than 2. For example, Wang *et al.*[6] reported (113) facets as being the most stable. These limitations, however, do not detract from the main goal of this work, which is to identify the trends in the atomistics of the faceting-defaceting transition (to be discussed below).

C. Spherical vs faceted NC

In the third step, we actually simulate NC embedded in a-SiO_2, which either have the shape predicted by the Wulff construction or are spherical and nonfaceted, and we address their relative stability. For this purpose, four cells were generated. Two of them contain NC which are originally constructed to be faceted with sizes ~3 and ~5 nm (hereafter called F1 and F2, respectively.) The other two contain NC which are spherical with the same sizes (called S1 and S2). The larger size (5 nm) corresponds to the lower limit for which faceted NC have been reported experimentally.[5,6] The number of atoms in the large (small) NC is ~1700 (800), while the total number of atoms in the whole structures are ~14 200 (6700). We took care so that the total Si content in all cases is the same, ~41%, to ensure similar oxide embedding environments.

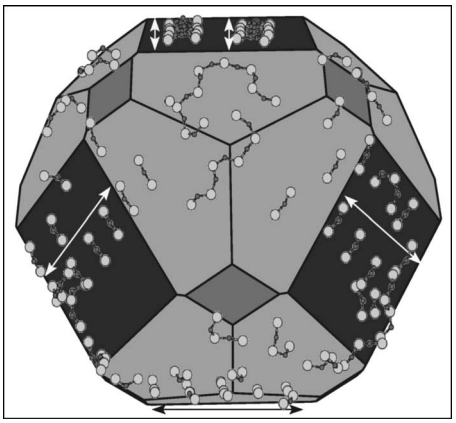

FIG. 2. The equilibrium shape which a Si-NC would have, if embedded, as obtained by using the Wulff construction and the face energies of Table I (absolute values). Dark gray, gray, and light gray denote the (100), (110), and (121) facets, respectively. Also shown is the distribution of Si-O-Si bridge bonds on the facets of the F2 Si-NC (see text). The embedding oxide is not shown.

Ball and stick models of the two originally faceted NC F1 and F2, after full relaxation and equilibration in the oxide, are shown in Fig. 3. Strikingly, while the larger NC (F2) retains its faceted polyhedral shape, the smaller one (F1) fails to keep its facets intact and finally obtains a spherical shape. This is reflected in the relative interface energies between the four cells (calculated in the same way as in the planar case). For S2, we find E_{inter} to be 0.066 eV/Å^2, compared to 0.052 eV/Å^2 for F2. The drop by 0.014 eV/Å^2 shows that the faceted shape for the large NC indeed is the thermodynamically stable phase. To the contrary, for the small size, we find that S1 has significantly lower energy (0.073 eV/Å^2) than the unrelaxed F1 (0.092 eV/Å^2), which explains the defaceting. After relaxation, F1 lowers its energy to 0.076 eV/Å^2 approaching that of S1. However, S1 has a higher energy than both the larger NC, S2, and F2 as expected.[8]

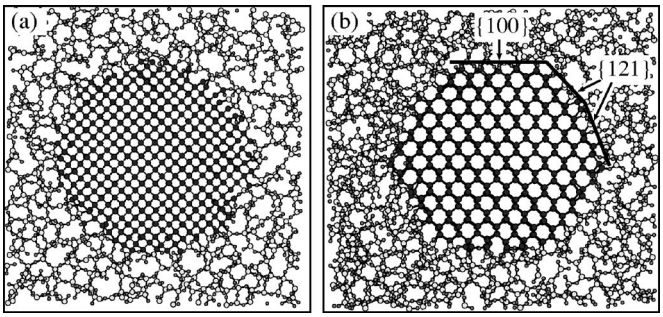

FIG. 3. Ball and stick models of the equilibrated structures of two originally faceted embedded NC. (a) F1 and (b) F2 (see text). Dark spheres show Si atoms in the NC. Large (small) grey spheres show Si (O) atoms in the oxide. In (b) the (100) and the (121) planes are clearly distinguished.

Further insight into the faceting-defaceting transition is obtained by analyzing the atomistic picture of the interface. We first note that all four interfaces have about the same suboxide component ratios, indicating that chemical disorder is not the main contributor to the transition. Another factor is the percentage of bridge bonds, which are low-energy elements at the interface.[8] We find that S1 has 63% bridges, while F1 has 50%, which might explain the drop in energy. However, S2 also has more bridges (66%) than F2 (54%), but it is higher in energy. Simply, spherical NC have on average more bridges than faceted ones, because some facets, such as (110), do not favor bridge formation. Thus, mere percentage of bridge bonds is not enough to explain the effect.

It turns out that the main contributor to defaceting is the increasing distortion of bridge bonds as the size gets smaller, raising up their energy. We find that the average bridge energy E_{bridge} is 0.33 eV for F2, compared to 0.42 eV for S2, while it is 0.67 eV for the unrelaxed F1 and 0.38 eV for S1, a 0.3 eV gain in energy when the NC defacets. A look at the way bridges are distributed on the facets of a NC reveals the origin of distortions. Figure 2 shows such an analysis for F2. Expectedly, the (100) facet has more bridges, in both the stripe and check phases,[11] a remnant from the infinite planar interface. Fewer bridges are formed on the (121) and even fewer on the (110) facets. Note that bridges on (121) join to form chains, fewer on (100), which frequently cross over the edges and apeces connecting two or three different facets.

This has a paramount effect on the energetics. For large NC, bridges are less distorted when formed on facets, because of the relatively large facet areas. However, as the size shrinks, especially below a critical size, which we estimate to be $\sim$4 nm, facet areas become too small and the contribution of edges and apeces, at which much of the stress is concentrated, becomes pronounced. Therefore, bridges on the edges get very distorted. For example, for F1, the energy of bridges on edges (facets) is 0.76 (0.42) eV. As most of the bridges lie close or on edges, the NC prefers to defacet and attain a spherical interface, on which bridge bonds have a lower energy.

Note that distortions in the transition region of 4–6 nm are concentrated at the NC interface, being minimal in the interior, contrary to what happens in NC smaller than 3 nm.[8] Thus, defaceting is driven by bond distortions at the interface and is not affected by the inner stress state of the NC.

Considering that the simulated Si-NC reach equilibrium, it follows that large spherical NC observed in experimental studies are in a metastable state. Although we cannot deduce from the present simulations the origin of this metastability, it is likely that kinetic constraints inhibit the development of well defined facets. An open issue for further investigation is the role of faceting and its influence on the doping and photoluminescence efficiency of Si-NC, as shown to be the case for II-VI nanocrystals.[2]

Another issue raised in the literature[14] concerns the role of structural defects, such as dangling bonds, in affecting the optical properties of isolated Si-NC. It was shown that H can passivate these defects, improving the optical emission. H passivation could in principle also be possible in embedded Si-NC. Unfortunately, the present simulations can not deal with this issue since only defect-free networks with fully bonded Si and O atoms can be simulated within the employed MC methodology. This limitation does not allow us to investigate whether dangling bonds play a role in the defaceting transition, especially in deciding the transition size. It is an interesting possibility which needs investigation.

In a more extensive study, one could simulate a larger number of initial configurations, having possibly facets with indices higher than 2, in order to describe more accurately the quantitative features of the problem, such as the transition size of the NC. However, we do not expect any change in the qualitative predictions of this work. The trends and origins of the faceting-defaceting transition, i.e., bond distortions at the edges/apeces, are common to all possible facet orientations.

Finally, it would be worthwhile to examine in the future whether the onset of faceting-defaceting transitions due to bond distortions at the edges/apeces of facets is a more general effect, relevant to other phenomena as well. For example, Wang *et al.*[13] observed that gold clusters soften below the bulk melting temperature *via* diffusion of atoms at first the vertices and then the edges of the cluster surface, as temperature is increased, so that the average shape of the cluster is nearly spherical at the melting transition. This observation might be connected to the findings of our work, but in order to be established a detailed study of the sequence of configurations involved in the defaceting transition is needed. This is beyond the scope of the present work, but it will be the subject of further studies.

IV. CONCLUSIONS

In conclusion, using MC simulations and the Wulff construction method, we have shown that faceting is the equilibrium state of large Si-NC embedded in a-SiO_2, and unraveled the atomistic mechanisms which lead to the destabilization of facets with shrinking NC size. The distortions of bridge bonds is the driving force for the defaceting, while chemical disorder plays a minor role. Open issues include the role of structural defects in influencing the transition, the role of faceting in increasing the doping efficiency of Si-NC, and a closer look at the intermediate configurations involved in the defaceting transition.

ACKNOWLEDGMENTS

This work is supported by a grant from the EU and the Ministry of National Education and Religious Affairs of Greece through the action "ΕΠΕΑΕΚ" (programme "ΗΡΑΚΛΕΙΤΟΣ"), and by a Greece-Cyprus bilateral grant from the General Secretariat for Research and Technology of Greece.

[1] X. Peng, L. Manna, W. Yang, J. Wickham, E. Scher, A. Kadavanich, and A. P. Alivisatos, Nature (London) **404**, 59 (2000).
[2] S. C. Erwin, L. Zu, M. I. Haftel, A. L. Efros, T. A. Kennedy, and D. J. Norris, Nature (London) **436**, 91 (2005).
[3] L. Pavesi, L. Dal Negro, C. Mazzoleni, G. Franzo, and F. Priolo, Nature (London) **408**, 440 (2000).
[4] S. Tiwari, F. Rana, K. Chan, L. Shi, and H. Hanafi, Appl. Phys. Lett. **69**, 1232 (1996); E. Kapetanakis, P. Normand, D. Tsoukalas, and K. Beltsios, *ibid.* **80**, 2794 (2002).
[5] Y. Ishikawa, N. Shibata, and S. Fukatsu, Appl. Phys. Lett. **68**, 2249 (1996).
[6] Y. Q. Wang, R. Smirani, and G. G. Ross, Nano Lett. **4**, 2041 (2004); Y. Q. Wang, R. Smirani, F. Schiettekatte, and G. G. Ross, Chem. Phys. Lett. **409**, 129 (2005).
[7] P. Normand, D. Tsoukalas, E. Kapetanakis, J. A. Van Den Berg, D. G. Armour, J. Stoemenos, and C. Vieud, Electrochem. Solid-State Lett. **1**, 88 (1998).
[8] G. Hadjisavvas and P. C. Kelires, Phys. Rev. Lett. **93**, 226104 (2004).
[9] Y. Tu and J. Tersoff, Phys. Rev. Lett. **84**, 4393 (2000); , Phys. Rev. Lett. **89**, 086102 (2002).
[10] F. Wooten, K. Winer, and D. Weaire, Phys. Rev. Lett. **54**, 1392 (1985).
[11] R. Buczko, S. J. Pennycook, and S. T. Pantelides, Phys. Rev. Lett. **84**, 943 (2000).
[12] G. Wulff, Z. Kristallogr. Mineral. **34**, 449 (1901); C. Herring, Phys. Rev. **82**, 87 (1951).
[13] Y. Wang, S. Teitel, and C. Dellago, J. Chem. Phys. **122**, 214722 (2005).
[14] S. Cheylan, and R. G. Elliman, Appl. Phys. Lett. **78**, 1225 (2001).